

# Dielectric Charging of RF MEMS Capacitive Switches under Bipolar Control-Voltage Waveforms

Zhen Peng, *Student Member, IEEE*, Xiaobin Yuan, *Member, IEEE*, James C. M. Hwang, *Fellow, IEEE*, David I. Forehand, *Member, IEEE*, and Charles L. Goldsmith, *Senior Member, IEEE*

**Abstract** — Bipolar control-voltage waveforms have been proposed to mitigate dielectric charging in RF MEMS capacitive switches. In this work, for the first time, dielectric charging under bipolar waveforms is modeled and characterized quantitatively. In general, the experimental results agree with predictions based on the superposition of charging models that are extracted under either positive or negative voltage only. The present analysis indicates that, while bipolar waveforms can reduce charging, it is difficult to fine tune the waveforms to completely eliminate charging.

**Index Terms** — Charge injection, dielectric films, dielectric materials, microelectromechanical devices, switches.

## I. INTRODUCTION

Currently, the life time of RF MEMS capacitive switches is mainly limited by dielectric charging [1]-[22]. To mitigate the charging problem, complex control-voltage waveforms, such as high-low and bipolar waveforms, have been proposed [1], [2]. In practice, charging under high-low waveforms was modeled and characterized [18] with beneficial results. Charging under bipolar waveforms is modeled and characterized, for the first time, in this work. The present model is based on the superposition of unipolar charging models [18] that are extracted under either positive or negative voltage only. In spite of the simplification through superposition, the model predictions are in general agreement with bipolar charging experiments under different switching frequencies, voltages, and duty factors.

The present RF MEMS capacitive switches are similar to that of [18]. The dielectric is sputtered SiO<sub>2</sub> with a thickness of 0.3 μm and a dielectric constant of 5.5. The top electrode is a moveable 0.3-μm-thick Al membrane that is grounded. The bottom Cr/Au electrode serves as the center conductor of a 50-Ω coplanar waveguide for the RF signal. Without any electrostatic force, the Al membrane is normally suspended in

Manuscript submitted on Dec. 1, 2006. Work was partially supported by the US Air Force Research Laboratory under Contract No. F33615-03-C-7003. The contract was funded by the US Defense Advanced Research Projects Agency under the Harsh Environment, Robust Micromechanical Technology (HERMIT) program.

Z. Peng, and J. C. M. Hwang are with Lehigh University, Bethlehem, PA 18015 USA. Z. Peng can be contacted at (610) 758-5109 or zhp205@lehigh.edu.

X. Yuan is with IBM, Hopewell Junction, NY 12533 USA

D. Forehand and C. Goldsmith are with MEMtronics Corp., Plano, TX 75075 USA.

TABLE I  
EXTRACTED MODEL PARAMETERS

Positive Voltage				
$J$	$Q_{00+}$ (g/cm <sup>2</sup> )	$V_{0+}$ (V)	$\tau_{C+}$ (s)	$\tau_{D+}$ (s)
1	$5 \times 10^9$	12	10	15
2	$9 \times 10^9$	10	65	130
Negative Voltage				
$J$	$Q_{00-}$ (g/cm <sup>2</sup> )	$V_{0-}$ (V)	$\tau_{C-}$ (s)	$\tau_{D-}$ (s)
1	$-2.5 \times 10^9$	10	8	13
2	$-7.5 \times 10^9$	10	60	114

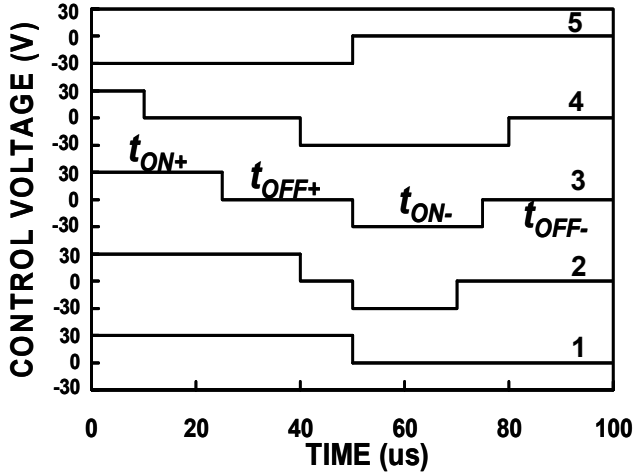
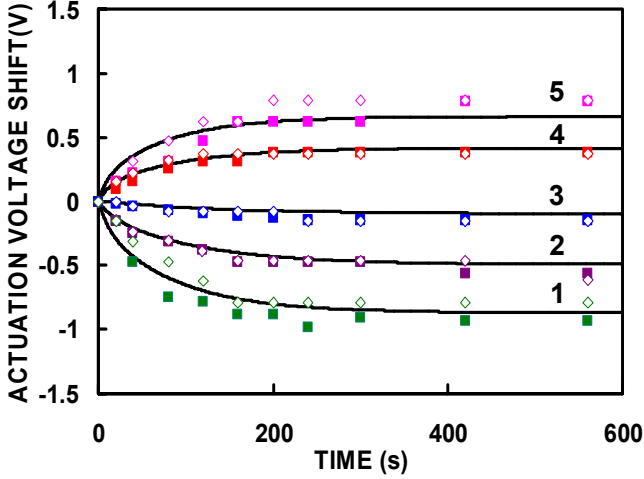
air 2.2 μm above the dielectric. A control voltage, either positive or negative, is applied to the bottom electrode, which pulls the membrane in contact with the SiO<sub>2</sub> thus forming a 120 μm x 80 μm capacitor to shunt the RF signal to ground. This results in low insertion loss (0.06 dB) at the off (membrane up) state and high isolation (15 dB) at the on (membrane down) state at 35 GHz. The pull-down or actuation voltage is typically ±25 V, while the release voltage is typically ±10 V. The switching time is less than 10 μs.

## II. MODEL CONSTRUCTION

Control voltages up to ±40 V were used to accelerate charging. The voltages are high enough to cause charge injection from the bottom electrode into the dielectric, yet low enough to avoid charge injection from the top electrode into the dielectric. (The top-charging threshold is approximately ±50 V [22].) Thus, under a positive control voltage, positive charge is injected from the bottom electrode into the dielectric, which gradually decreases the actuation voltage from 25 to, say, 24 V. On the other hand, under a negative control voltage, negative charge is injected from the bottom electrode into the dielectric, which gradually increases the actuation voltage from •25 to, say, •24 V. Therefore, depending on the sign of the control voltage, bottom charging can be either positive or negative but always changes the actuation voltage  $V$  according to the following [18]:

$$\Delta V = -hQ / \epsilon, \quad (1)$$

where the electrostatic effect of the charge is approximated by a sheet charge of density  $Q$  located at height  $h$  above the bottom electrode, and  $\epsilon$  is the dielectric constant. A single  $h$



(b)

Fig. 1. (a) (line) Modeled vs. (symbol) measured actuation-voltage shifts under control-voltage waveforms No. 1 to No. 5 (Table II) at (■) 10 Hz and (◇) 10 kHz and illustrated in (b).

value of  $0.12 \mu\text{m}$  was found to give the best fit between model predictions and experimental data under all control waveforms.

Following [18], unipolar charging behaviors under positive and negative voltages were separately characterized. Based on the measured transient charging and discharging currents, the accumulated charge can be fitted with the sum of two exponential terms:

$$Q_{\pm} = \sum_{J=1,2} Q_{0,J\pm} (1 - e^{-\frac{t_{ON\pm}}{\tau_{CJ\pm}}} - e^{-\frac{t_{OFF\pm}}{\tau_{DJ\pm}}}), \quad (2)$$

where subscripts “+” and “•” denote charging under positive and negative voltages, respectively;  $Q_{0J}$  is the steady-state charge density;  $t_{ON}$  and  $t_{OFF}$  are on and off times of the switch;

TABLE II  
CONTROL-VOLTAGE WAVEFORMS

No.	$V_+$ (V)	$V_-$ (V)	$t_{ON+}$ ( $\mu\text{s}$ )	$t_{OFF+}$ ( $\mu\text{s}$ )	$t_{ON-}$ ( $\mu\text{s}$ )	$t_{ON-}$ ( $\mu\text{s}$ )
1	30	--	50	50	--	--
2	30	-30	40	10	20	30
3			25	25	25	25
4			10	30	40	20
5	--	-30	--	--	50	50
6	35	-35	10	30	40	20
7	40	-40				
8	35	-30				
9	30	-35				

$\tau_c$  and  $\tau_d$  are charging and discharging time constants. Usually,  $Q_+ > 0$  and  $Q_- < 0$ .

The steady-state charge density was found to increase exponentially with voltage, so that

$$Q_{0,J\pm} = Q_{00,J\pm} e^{V_0/J\pm}, \quad (3)$$

where  $Q_{00}$  is a pre-exponential factor and  $V_0$  is a voltage scaling factor. Table I lists the fitted values of  $Q_{00}$ ,  $V_0$ ,  $\tau_c$  and  $\tau_d$ . Notice that, except for the sign of  $Q_{00}$ , the values are very similar under positive and negative voltages. This implies that a symmetrical bipolar waveform should have minimum charging.

Table II lists the various control-voltage waveforms that are illustrated in Fig. 1(b). For example, at a switching frequency of 10 KHz, each switching cycle  $\Delta t = t_{ON+} + t_{OFF+} + t_{ON-} + t_{OFF-} = 100 \mu\text{s}$ . After several cycles, a small amount of charge  $Q(t)$  may accumulate due to the subtle difference between positive and negative charging behaviors. Assuming  $Q(t) > 0$ , (2) can be used to evaluate charging during the next switching cycle:

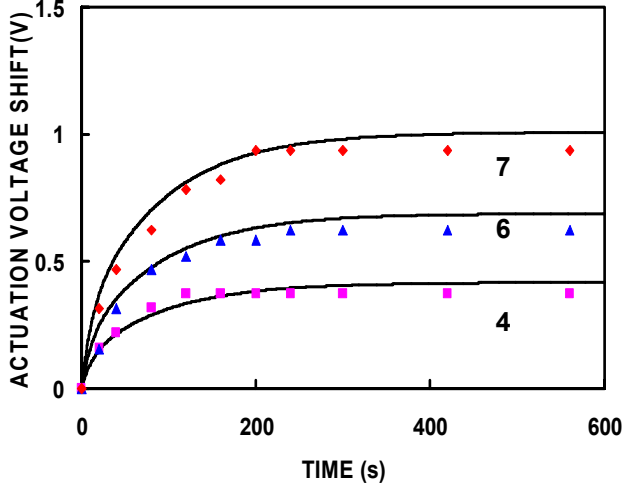
$$Q(t + t_{ON+}) = Q(t) e^{-\frac{t_{ON+}}{\tau_{C+}}} + Q_{0+} (1 - e^{-\frac{t_{ON+}}{\tau_{C+}}}), \quad (4)$$

where the summation over the subscript  $J = 1$  and  $2$  is omitted for clarity. Subsequently,

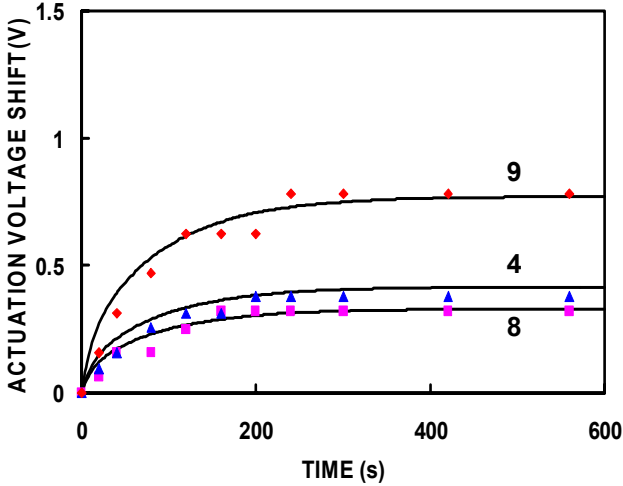
$$Q(t + t_{ON+} + t_{OFF+}) = Q(t + t_{ON+}) e^{-\frac{t_{OFF+}}{\tau_{D+}}}, \quad (5)$$

$$Q(t + t_{ON+} + t_{OFF+} + t_{ON-}) = Q(t + t_{ON+} + t_{OFF+}) e^{-\frac{t_{ON-}}{\tau_{D+}}} + Q_{0-} (1 - e^{-\frac{t_{ON-}}{\tau_{C-}}}), \quad (6)$$

where we assume discharging of the positive charge under a negative voltage is the same as that without any voltage, and negative charging is unaffected by the accumulated positive charge. Finally,



(a)



(b)

Fig. 2. (line) Modeled vs. (symbol) measured actuation-voltage shifts under control-voltage waveforms (a) 4, 6 and 7 and (b) 4, 8 and 9 as listed in Table II. The switching frequency is 10 kHz.

$$Q(t + \Delta t) = Q(t + t_{ON+} + t_{OFF+} + t_{ON-}) e^{-\frac{t_{OFF+}}{\tau_{D+}}} \quad (7)$$

Starting with  $Q(0) = 0$ , (4)-(7) can then be iterated  $n$  times to determine  $Q(n\Delta t)$ .

If  $Q(t) < 0$ , then it is more convenient to start with negative charging during the second half of the bipolar switching cycle so that (4)-(7) can be duplicated except for sign change. Thus,

$$Q(t + t_{ON-}) = Q(t) e^{-\frac{t_{ON-}}{\tau_{C-}}} + Q_{0-} (1 - e^{-\frac{t_{ON-}}{\tau_{C-}}}), \quad (8)$$

$$Q(t + t_{ON-} + t_{OFF-}) = Q(t + t_{ON-}) e^{-\frac{t_{OFF-}}{\tau_{D-}}}, \quad (9)$$

$$Q(t + t_{ON-} + t_{OFF-} + t_{ON+}) = Q(t + t_{ON-} + t_{OFF-}) e^{-\frac{t_{ON+}}{\tau_{D-}}} + Q_{0+} (1 - e^{-\frac{t_{ON+}}{\tau_{C+}}}), \quad (10)$$

$$Q(t + \Delta t) = Q(t + t_{ON-} + t_{OFF-} + t_{ON+}) e^{-\frac{t_{OFF+}}{\tau_{D+}}}. \quad (11)$$

Once  $Q$  is found through iterations of (4)-(7) or (8)-(11), (1) can be used to determine the actuation-voltage shift.

### III. RESULTS AND DISCUSSION

Using previously developed [18] test setup and procedure, actuation-voltage shifts under different waveforms were measured and compared with model predictions as shown in Figs. 1 and 2. Agreement was found for different switching frequencies, voltages, and duty factors. The principle of superposition applies to the present Cr-SiO<sub>2</sub>-Al capacitors probably because they have similar charging behaviors under both positive and negative voltages, and there appears to be no strong interaction between positive charging and negative charging. Similar to unipolar charging [18], bipolar charging, although of smaller magnitude, increases with stress time and voltage, but is independent of switching frequency as long as the switching cycle is much shorter than charging/ discharging time constants.

As mentioned before, due to the subtle difference between positive and negative charging, a small amount of charge gradually accumulates even under a symmetrical bipolar waveform (No. 3). Thus, it is tempting to fine tune the waveform in order to exactly balance out positive and negative charging within each switching cycle. This implies that

$$Q_{0+} (1 - e^{-\frac{t_{ON+}}{\tau_{C+}}}) e^{-\frac{t_{OFF+} + t_{ON-}}{\tau_{D+}}} = Q_{0-} (1 - e^{-\frac{t_{ON-}}{\tau_{C-}}}). \quad (12)$$

Usually, the switching cycle is much shorter than charging/discharging time constants. Therefore,

$$Q_{0+} t_{ON+} / \tau_{C+} \cong Q_{0-} t_{ON-} / \tau_{C-} \quad (13)$$

or

$$t_{ON+} / t_{ON-} \cong Q_{0-} \tau_{C+} / Q_{0+} \tau_{C-}. \quad (14)$$

Thus, to exactly cancel charging within each bipolar switching cycle, the on times of positive and negative voltages need to be fine tuned according to (14). If the application requires  $t_{ON+}$  and  $t_{ON-}$  to be equal, then

$$Q_{0+} / Q_{0-} \cong \tau_{C+} / \tau_{C-}. \quad (15)$$

From (3),

$$Q_{00+} \exp(V_+ / V_{0+}) / Q_{00-} \exp(V_- / V_{0-}) \cong \tau_{C+} / \tau_{C-}. \quad (16)$$

Since  $Q_{0+} \sim Q_{00}$  and  $\tau_{c+} \sim \tau_{c-}$ ,

$$V_+ / V_- \equiv V_{0+} / V_{0-}. \quad (17)$$

However, (17) is difficult to satisfy precisely due to the exponential voltage dependence of (16), especially if second-order terms are included in the summation over  $J$ .

## VI. CONCLUSION

In conclusion, bipolar control-voltage waveforms were found to reduce dielectric charging in RF MEMS capacitive switches. A bipolar charging model was developed from the superposition of unipolar charging models. The model agrees well with the experimental results obtained under bipolar waveforms of different frequencies, voltages, and duty factors. The model also shows that it is difficult to fine tune the waveform to completely eliminate charging.

## REFERENCES

- [1] C. Goldsmith, J. Ehmke, A. Malczewski, B. Pillans, S. Eshelman, Z. Yao, J. Brank, and M. Eberly, "Lifetime characterization of capacitive RF MEMS switches," *IEEE MTT-S Int. Microwave Symp. Dig.*, pp. 227-230, June 2001.
- [2] J. R. Reid, and R. T. Webster, "Measurements of charging in capacitive microelectromechanical switches," *Electron. Lett.*, vol. 38, no. 24, pp. 1544-1545, Nov. 2002.
- [3] W. M. van Spengen, R. Puers, R. Mertens, and I. De Wolf, "Experimental characterization of stiction due to charging in RF MEMS," *IEEE Int. Electron Devices Meet. Dig.*, pp. 901-904, Dec. 2002.
- [4] W. M. van Spengen, R. Puers, R. Mertens, and I. De Wolf, "A comprehensive model to predict the charging and reliability of capacitive RF MEMS switches," *J. Micromech. Microeng.*, vol. 14, pp. 514-521, Jan. 2004.
- [5] X. Yuan, S. V. Cherepko, J. C. M. Hwang, C. L. Goldsmith, C. Nordquist, and C. Dyck, "Initial observation and analysis of dielectric-charging effects on RF MEMS capacitive switches," *IEEE MTT-S Int. Microwave Symp. Dig.*, pp. 1943-1946, June 2004.
- [6] X. Rottenberg, B. Nauwelaers, W. Raedt, and H.A.C. Tilmans, "Distributed dielectric charging and its impact on RF-MEMS device," *GAAS 12<sup>th</sup> Symp. Dig.*, pp. 475-478, Oct. 2004.
- [7] X. Yuan, J. C. M. Hwang, D. Forehand, and C. L. Goldsmith, "Modeling and characterization of dielectric-charging effects in RF MEMS capacitive switches," *IEEE MTT-S Int. Microwave Symp. Dig.*, pp. 753-756, June 2005.
- [8] S. Melle, D. De Conto, L. Mazeng, D. Dubuc, K. Grenier, L. Bary, O. Vendier, J. L. Cazaux, and R. Plana, "Modeling of the dielectric charging kinetic for capacitive RF-MEMS," *IEEE MTT-S Int. Microwave Symp. Dig.*, pp. 757-760, June 2005.
- [9] G. J. Papaioannou, M. Exarchos, V. Theonas, G. Wang, and J. Papapolymerou, "On the dielectric polarization effects in capacitive RF-MEMS switches," *IEEE MTT-S Int. Microwave Symp. Dig.*, pp. 761-764, June 2005.
- [10] G. J. Papaioannou, M. Exarchos, V. Theonas, G. Wang, and J. Papapolymerou, "Temperature study of the dielectric polarization effects of capacitive RF-MEMS switches," *IEEE Trans. Microwave Theory Techniques*, vol. 53, no. 11, pp. 3467-3473, Nov. 2005.
- [11] S. Melle, D. De Conto, D. Dubuc, K. Grenier, O. Vendier, J. L. Muraro, J. L. Cazaux, and R. Plana, "Reliability modeling of capacitive RF MEMS," *IEEE Trans. Microwave Theory Techniques*, vol. 53, no. 11, pp. 3482-3488, Nov. 2005.
- [12] R. W. Herfst, H. G. A. Huizing, P. G. Steeneken, and J. Schrnitz, "Characterization of dielectric charging in RF MEMS capacitive switches," *Dig. IEEE Int. Conf. Microelectronic Test Structures*, pp. 133-136, Mar. 2006.
- [13] J. F. Keko, J. C. Petrosky, J. R. Reid, and K. Yung, "Non-charge related mechanism affecting capacitive MEMS switch lifetime," *IEEE Microwave Wireless Components Lett.*, vol. 16, no. 3, pp. 140-142, Mar. 2006.
- [14] S. Patton, and J. Zabinski, "Effects of dielectric charging on fundamental forces and reliability in capacitive microelectromechanical systems radio frequency switch contacts," *J. Appl. Phys.*, vol. 99, issue 9, pp. 1700-1710, May. 2006.
- [15] X. Yuan, Z. Peng, J. C. M. Hwang, D. Forehand, and C. L. Goldsmith, "Temperature Acceleration of dielectric-charging effects in RF MEMS capacitive switches," *IEEE MTT-S Int. Microwave Symp. Dig.*, pp. 47-50, June 2006.
- [16] G. J. Papaioannou, M. Exarchos, V. Theonas, J. Psychias, G. Konstantinidis, D. Vasilache, A. Muller, and D. Neculoiu, "Effect of space charge polarization in radio frequency microelectromechanical system capacitive switch dielectric charging," *Appl. Phys. Lett.*, vol. 89, issue 10, pp. 922-924, Sep. 2006.
- [17] D. Molinero, R. Comulada, and L. Castañer, "Dielectric charge measurements in capacitive microelectromechanical switches," *J. Appl. Phys.*, vol. 89, issue 8, pp. 901-903, Sep. 2006.
- [18] X. Yuan, Z. Peng, J. C. M. Hwang, D. Forehand, and C. L. Goldsmith, "A transient SPICE model for dielectric-charging effects in RF MEMS capacitive switches," *IEEE Trans. Electron Devices*, vol. 53, no. 10, pp. 2640-2648, Oct. 2006.
- [19] M. Exarchos, E. Papandreou, P. Pons, M. Lamhamdi, G. J. Papaioannou, and R. Plana, "Charging of radiation induced defects in RF MEMS dielectric films," *Microelectronics Reliability*, vol. 46, issue 9-11, pp. 1695-1699, Sep-Nov. 2006.
- [20] M. Lamhamdi, J. Guastavino, L. Boudou, Y. Segui, P. Pons, L. Bouscayrol, and R. Plana, "Charging-effects in RF capacitive switches influence of insulating layers composition," *Microelectronics Reliability*, vol. 46, issue 9-11, pp. 1700-1704, Sep-Nov. 2006.
- [21] X. Yuan, Z. Peng, J. C. M. Hwang, D. Forehand, and C. L. Goldsmith, "Acceleration of dielectric charging in RF MEMS capacitive switches," *IEEE Trans. Device Materials Reliability*, Dec. 2006.
- [22] Z. Peng, X. Yuan, J. C. M. Hwang, D. Forehand, and C. L. Goldsmith, "Top vs. bottom charging of dielectric in RF MEMS capacitive switches," *Proc. 2006 Asia Pacific Microwave Conf.*, Dec. 2006.